Time structure of light field
from a point source in scattering medium

G.P. Kokhanenko

Institute of Atmospheric Optics,
Siberian Branch of the Russian Academy of Sciences, Tomsk

Pulsed radiation undergoes distortions due to the multiple scattering effects while propagated through a layer of a scattering medium. This paper presents the results on the time shape of a pulse calculated numerically for the cases of media with different scattering phase functions. It is shown that even at rather large optical thickness ($\tau \approx 10-20$), time shape of scattered radiation pulse cannot be described using diffusion theories, being, as a rule, a bimodal distribution. Only at a significant increase in optical thickness ($\tau > 100-150$), the photon distribution over photon free paths takes a unimodal "diffusion" shape.

Introduction

Pulse light sources are widely used in optical communication and navigation, as well as in detection and ranging. Propagation of a light pulse through the scattering medium (such as atmosphere or water) is accompanied by multiple light scattering that causes pulse delay and thus increases its duration.

If optical thickness τ of the scattering layer is small ($\tau \ll 1$), a signal is determined by the direct and single-scattered radiation. In this case, the time pulse-width broadening is determined by the geometrical parameters of the experiment, namely, range, field-of-view angle, etc. Increase in τ causes the dominance of multiple scattering and dependence of a signal shape on optical parameters of the scattering medium such as optical thickness and asymmetry of the scattering phase function.

The most complicated shape of a signal is observed in the case of optical receivers with a wide field of view (illuminometers), since in this case, even at $\tau \ll 1$, the photons scattered at large angles make up a significant fraction of the total signal energy. These photons are delayed in time much stronger than the photons scattered at small angles. Consequently, radiation time structure (photon distribution over free paths) acquires a complex multimodal structure in the transient range of optical thickness (from $\tau \ll 1$ up to $\tau \gg 1$).

Analysis of the well-known experimental observations and numerical calculations conducted by the author show that time shape of an optical signal could not be uniquely determined under these conditions by the maximum delay or by the duration at half-maximum level. In this paper I present results on the photon distribution over free paths calculated for media with different asymmetry of the scattering phase function. One can observe the distribution transformation from multimodal to the "diffusion"

type at unlimited increase of the optical thickness of the scattering medium.

1. Pulse deformation in scattering media

Let us assume that there is a short light pulse $I_0\delta(r)\delta(t)$ in the scattering medium (may be, at its boundary). Direct attenuated radiation will reach the receiver placed in the medium at the point **r** ($|r| = Z$) at a time moment $T_0 = Z/c$, where c is the speed of light in the medium. Direct radiation intensity is attenuated exponentially

$$I(\mathbf{r},t) = I_0 \exp(-\tau)\delta(t - T_0)$$

while keeping the initial feature $\delta(t)$. (Here $\tau = \varepsilon Z$ is the optical thickness of the path, ε is the attenuation coefficient). The radiation of different scattering orders will produce a pulse in the detector whose maximum is delayed by $t_{\max}$ relative to the arrival time of the first photon and has the duration δt (the half-maximum level). At large values of τ the fraction of the attenuated direct flux is negligible and the recorded signal is determined mainly by the scattered radiation.

For the illuminometer (receiver with a unity aperture and cosine-type directional pattern), the recorded signal power $P(t)$ is related to the intensity $I(t)$ by the following expression

$$P(t) = \int\limits_{2\pi} I(t)\cos\varphi\,d\omega,$$

where φ is the angle of incidence, $d\omega$ is the element of solid angle. Time shape of a signal $P(t)$ can be interpreted as a distribution of photons over free paths $P(l = ct)$.

It is usually assumed that this distribution is rather simple, like Γ-distribution, with a steep front and slow droop and constant ratio between $t_{\max}$ and

　　　　　© 2006　Institute of Atmospheric Optics

δt. In this case the task is to estimate the time parameters (t_{max}, δt) of the pulse depending on optical parameters of the medium (such as optical thickness, τ, average cosine of the scattering angle, $<\cos\gamma>$, etc.).

In the general case, radiation intensity is determined by solution of the time-dependent radiation transfer equation (RTE)[1–4]:

$$\left(\frac{1}{c}\frac{\partial}{\partial t} + \mathbf{s}\nabla_r + \varepsilon\right) I(\mathbf{r},\mathbf{s},t) = \Lambda \int_{4\pi} g(\mathbf{s},\mathbf{s}')\, I(\mathbf{r},\mathbf{s}',t)\, d\omega. \quad (1)$$

Here $I(\mathbf{r},\mathbf{s},t)$ is the radiation intensity at the point $\mathbf{r}$ along direction of $\mathbf{s}$, $\Lambda = \sigma/\varepsilon$ is the single scattering albedo, σ is the scattering coefficient. The scattering phase function $g(\gamma)$ is normalized by the condition $\int_{4\pi} g(\gamma)\, d\omega = 1$, γ is the scattering angle. As a rule, one can obtain solutions of the time-dependent RTE from the corresponding approximation of a steady-state equation by applying the Laplace transform in time.[5] Unfortunately, analytical solutions are known only for a limited range of variation of the medium optical parameters (single scattering albedo, scattering phase function asymmetry), that leads to the additional restrictions on time interval where an unsteady solution is valid.

Asymptotic solutions of the time-dependent equation[6] are known that describe the light pulse shape at $t \to \infty$ for different geometry of the scattering medium. For example, for a point source in an infinite scattering medium considered in this paper, radiation intensity falls down according to the law $t^{-3/2}$ (Ref. 2). Media with noticeable true absorption and strongly forward peaked scattering phase function (for example, seawaters) well conform to the applicability conditions of the small-angle approximation,[7–9] allowing only for the scattering at small angles. The situation is more difficult with the scattering media having low true absorption (κ is much lower than σ), since the photons scattered at large angles make a significant contribution to the scattered radiation intensity at $t \to \infty$. Since such media are the subject of this study, we shall consider them in a more detail.

The brightness field in conservative media quite rapidly becomes close to isotropic as photons penetrate into the medium depth. Therefore, one can present the radiation propagation at large distances from the medium boundaries as a process of energy diffusion described by the diffusion equation[1,10,12]:

$$\frac{1}{c}\frac{dU}{dt} = D\nabla^2 U - \kappa U. \quad (2)$$

Here $U(\mathbf{r},t) = \int_{4\pi} I(\mathbf{r},\mathbf{s},t)\, d\omega$ is the average radiation intensity (spatial illumination), D is the diffusion coefficient.

Various approaches lead to the diffusion equation. Rather simple representations of scattering as a process of photon random walk through a grid of scattering centers, have allowed Chandrasekhar[10] to obtain the expression for the photon distribution over free paths for the case of isotropic scattering. Chandrasekhar has pointed out that in the asymptotic case of a great number of collisions ($Z/l \gg 1$, $l = 1/\sigma$ is the free path), the distribution is described by the diffusion equation with $D = 1/3\sigma$. For nonisotropic scattering, the diffusion equation conforms to the first approximation of the spherical harmonics method, moreover, the results of the isotropic scattering approach are applicable, if $l = 1/\sigma$ is replaced by the transport length $l_D = 1/\sigma(1 - <\cos\gamma>)$.[11,12] This typical dimensionless parameter calls for diffusion (transport) optical path length $\tau_D = \sigma Z(1 - <\cos\gamma>)$. Quite detailed solutions of the RTE for unsteady state radiation were obtained in diffusion approximation (DA) in 70s by Zege[13] and Ivanov,[14] and by Ishimaru, Ito, Furutsu, and Chevro,[15–19] in 80s and 90s of the 20th century. The process of photon random walk was considered in Ref. 20.

Another diffusion state of light field is observed at $\tau = \sigma Z$, in the case of strongly forward peaked scattering phase function, when angular variance of the radiation beam $<\theta^2>$ is, as in DA, much larger than the single scattering variance $<\gamma^2>$ owing not to the large optical thickness, but to the smallness of $<\gamma^2>$: $1 \ll <\gamma^2> \ll <\theta^2>$ (small-angle diffusion approximation, SDA). Solutions in SDA for wide and narrow beams have been obtained by Dolin,[21] Remizovich,[22] and Rogozkin.[23] The SDA gives satisfactory results on radiation time shape allowing for the dependence of D on the time of photon residence in the medium.[23–25]

For the diffusion radiation (normal spatial distribution and angular one close to isotropic), the photon distribution over free paths has quite a simple shape with a steep front and a power-law falloff. It is just for this case, that it is possible to construct a unique representation for time (and angular and spatial) distribution of the brightness field in terms of its known moments (first and second).[26] Similar approach was realized, in particular, by McLean[27] who regenerated the pulse shapes up to $\tau = 24$, applying the SDA formulas[23] and the moments calculated by Lutomirskii.[28] In the general case, knowledge of the field moments gives no unique representation of exact shape of the photon distribution over free paths.

The idea that pulse spreading is caused by radiation diffusion in the scattering medium is clear from the physical point of view and allows one to use DAs at large optical thickness ($\tau_D \gg 1$). At smaller τ the radiation time structure can be quite different. In comparing our numerical results with those predicted by DAs, we shall use the formula for a signal power proposed by Ito and Furutsu[16,18]:

$$P(t) = \frac{\sigma^3 c}{8\pi^{3/2}} \frac{\eta^{3/2}}{(\sigma c t)^{3/2}} \exp\left(-\frac{\eta\tau^2}{4\sigma c t}\right). \quad (3)$$

Here $\eta = 3(1 - \langle\cos\gamma\rangle)$. The formula was obtained for the scattering layer illuminated by a broad radiation beam and has the same asymptotic behavior of a signal ($t^{-3/2}$) as in the case with a point source. For the case of a narrow directed beam of radiation when the transverse radiation diffusion is essential, the pulse droop will be more rapid.[18,50] From Eq. (3) one obtains for δt and t_{max} the following estimates

$$\delta u \equiv \sigma c\delta t \approx \eta\tau^2/2; \ t_{max} \approx \delta t/3. \tag{4}$$

Proportionality of the delay time to the squared optical thickness is typical for the process of photon walks random in the scattering medium.[10,14,49] If the scattering layer was limited in space, the influence of boundary conditions would lead to the small deviation from the quadratic dependence at small τ.[14,19]

2. Analysis of experimental observations of the light pulses

In order to elucidate the applicability of the approximate solutions of the RTE under different conditions, it is necessary to compare the analytically calculated results with the results of field or numerical experiments. Obvious advantages of the numerical modeling are that the medium optical parameters and geometry of the experiment can be set precisely. However, there are only few calculations of the pulse time broadening and this is because, first, of certain difficulties in getting a representative statistical data on media with high scattering anisotropy using fine time grid. Let us mention only some studies.[25,29–35] Certain simplifications of the experimental arrangement have been used in many studies, for example, a limited time resolution[33] or the account of the forward scattering[31] only. It should be noted that limited potentialities of computers in 1970−1980 years did not allow obtaining the calculation statistics sufficient for solving time-dependent problems.

Such situation explains the attention of the researchers to the experimental studies. In 1970s and 1980s, a number of observations was performed of time broadening of light pulses propagated through scattering media both in field and under model conditions.[36–47] Some information about these observations is presented in the Table.

Experimental observations of light pulses in scattering media

Refs.	Range	Time resolution of the recorder	Field of view angle 2φ, deg	Optical thickness	Maximum broadening
41	11 cm	25 ps	16—36	13—77	690 ps
43	4 m	1 ns	60	20—50	6 ns
47	20 m	0.5 ns	2	10—80	42 ns
45	100 m	2 ns	10	25	60 ns
40	0.96 km	20 ns	2—15	18—30	175 ns
42	1.2 km	10 ns	0.5	8—20	22 ns
37	2 km	30 ns	5—20	4—25	0.6 µs
36	7.2 km	50 ns	4	34—249	15 µs
39	12 km	200 ns	4—34	30—50	20 µs
38	13.6 km	150 ns	0.01—1	4—12	0.5 µs

The experiments essentially differed by the path length and time resolution of the receiving equipment. There were long paths about 7 to 13 km (Mooradian,[39] Bucher and Lerner,[36] Paik[38]) and model chambers with the paths of 11 cm (Elliott[41]) to 20 m (Vergun[47]) length. As a rule, water fogs and clouds were observed in the experiment. The exceptions are a series of studies by Gol'din and Pelevin[44,45] in natural ocean waters and experiments in the Elliott model chamber,[41] where paraffin suspension in the water was one of the media. In most cases, when a considerable pulse broadening was observed the signals had shapes close to that caused by diffusion, i.e., these had a steep front edge and quite a slow falloff. Mooradian[39] had distinguished two Γ-distributions in a signal, differing by duration approximately triply, and had attributed the narrower one to the low-orders of scattering. Leelavathi[48] explained it by the simultaneous three-dimensional and one-dimensional diffusions and discovered the same pattern in data obtained by Elliott.[41] In some experiments, we have observed the dependence of a signal shape on the field-of-view (FOV) angle of the receiver, however the pulse duration varied by 3 to 5 times while changing the FOV angle from 2 to 35° (Refs. 39—41, 47). Weak dependence of pulse duration on FOV was shown by Chievro[19] using a diffusion approach.

The measured pulse durations considerably differed in the above-mentioned studies, however, the matter was not only in different path lengths. Bucher and Lerner[36] observed the broadening up to 32 µs at a range of 7.2 km at FOV equal 4°, whereas Paik,[38] with his path of 13.6 km length and 1° FOV did not observe any considerable broadening at the same 150-ns time resolution of the recorder. It is important for our analysis that in some experiments, (Elliott[41] at $\tau_D < 3.1$, Mooradian[40] at $\tau = 20$, Matter[42] in measurements on the beam axis) peaks were observed in the beginning of pulses along with the diffusion radiation and that the peaks' duration did not exceed time resolution of the recorders. Energy of these peaks considerably exceeded direct beam energy (exponentially attenuated), therefore, these pulses were, quite naturally, interpreted to be caused by the fraction of radiation multiply scattered along the forward direction at angles within the limits of the receiver's FOV. The similar peaks were also calculated in numerical simulations.[30]

Great variety of conditions (geometrical and optical) realized in the experiment, does not allow one to compare correctly all measured angular, spatial, and energy distributions. However, one can analyze the time broadening of the pulses based on predictions by diffusion theories, since the time broadening at rather large optical thicknesses is not sensitive to the medium stratification, and the scattering properties are preset by the single parameter, i.e., by the mean cosine of scattering angles.

Experimental data on measured pulse time broadening obtained in the above-discussed studies are shown in Fig. 1.

Naturally, only durations of the "diffusion" component of a signal are presented, since the finite time resolution of the recorder didn't allow accurate time shape of the multiply scattered forward radiation (if it was recorded) to be measured. The horizontal axis in Fig. 1 shows optical thickness of the scattering layer, the vertical axis presents the value $\eta' = \delta u/\tau^2$, which, according to Eq. (4), should depend only on the asymmetry of the medium scattering phase function. The dashed curves *13* and *14* show the dependences of the pulse duration for broad and narrow beams obtained using DA[18] with regard for the boundary conditions. In some data, the variation limits of duration are marked (vertical arrows), which were observed at FOV change. The measurement errors in the duration and optical thickness are presented if those were given in the above-quoted papers. It should be noted that no optical thickness value was not given in two papers[37,39] and I estimated it based on the indirect information.

Experimental data on the duration obtained in the scattering media different than the water fog were recalculated by Eq. (4) in correspondence with the value of $<\cos\gamma>$ taken from Refs. 41 and 45.
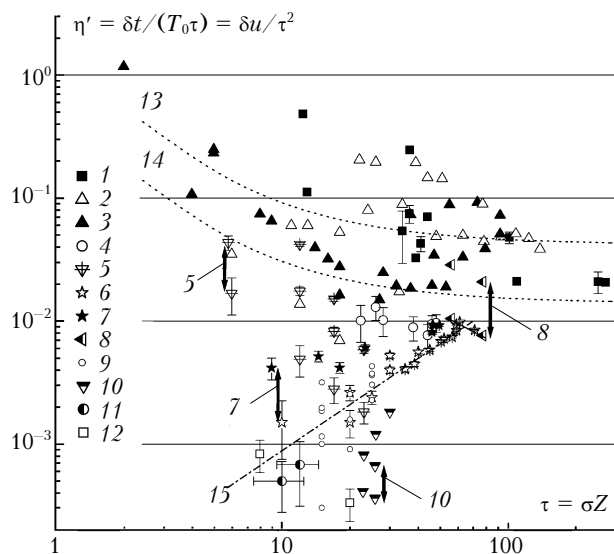

Fig. 1. Experimentally observed time broadening of light pulse. Digits correspond to the references: (*1*) Ref. 36; (*2, 3*) Ref. 41 for different scattering media; (*4*) Ref. 43; (*5*) Ref. 45; (*6, 7*) Ref. 47 for two polarization components; (*8*) Ref. 39; (*9*) Ref. 37; (*10*) Ref. 40; (*11*) Ref. 38; (*12*) Ref. 42.

First it is seen that some data[36,41] well agree with the dependence predicted by DA. At the same time, some data have a completely different, stronger than quadratic dependence of the duration on the optical thickness (for example, the author's data[47] shown by the dashed-dotted curve *15*). In the range of transient optical thickness $\tau = 10-30$ (already $\tau \gg 1$, but $\tau_D = \tau(1 - <\cos\gamma>)$ is not large yet), the spread measurement data obtained by different authors makes three orders of magnitude. No diffusion

theories can explain such a spread by the effect of experimental conditions (FOV angles, cross size of the scattering layer, etc.). Obviously, the definition of the pulse duration as the width at half-maximum used in the experiment does not work correctly. This occurs because it is impossible to present the "diffusion" component of the radiation using a unimodal Γ-distribution.

Based on the data of model experiments and numerically calculated results, we have assumed (see Refs. 24 and 35) that, actually, pulse shape (distribution of photons over free paths) in the region of transient optical thickness is as bimodal (or higher modality) distribution of the type presented below (see Section 4). The first group of photons (photons of attenuated direct beam and photons multiply scattered forward) conserves the initial $\delta(t)$ feature. The photons scattered at small-angles have though insignificant, but finite, duration and their distribution takes nearly asymptotic falloff rate. However, the "tail" of this distribution does not approach the real asymptotic.

Diffuse background formed by photons multiply scattered at large-angles having thus "forgotten" directions of the initial motion forms its own distribution different from the adjacent one both in time and power. A fraction of energy of each of these photon groups depends, first, on such parameters as optical thickness of the medium and asymmetry of the scattering phase function. Not a real experiments could provide has such a wide dynamic range (both in time and power), that would enable one to record simultaneously the adjacent maxima of the radiation. The result strongly depends on time resolution of the recorder. In the case of low resolution (compared to the path length) the real diffuse maximum is recorded and everything scattered at small-angles is interpreted as a peak of formed by radiation multiply scattered forward. Sufficiently high time resolution allows accurate recording of the time behavior of radiation scattered at small-angles and it is considered that this is the "diffuse" maximum whereas the true diffuse maximum has much lower power, by several orders of magnitude being usually masked by the instrumental noise.

Interpretation of observations at narrow FOV of the receiver is of a special difficulty, as the distribution peak has the delta shape. In this case, the definition of pulse duration as the distribution width at half-maximum becomes meaningless, and the pulse shape observed in the experiment is entirely determined by time resolution of the recorder.

At $(\tau_D \to \infty)$, a similar multimodal pulse structure should smoothly transfer into the distribution having true diffusion shape. As follows from Fig. 1, the measurement ambiguities disappear at the optical thickness about 100 ($\tau_D \approx 10$). Below I shall show, by means of numerical modeling, fine details of the time behavior of the light field from a point source in a homogeneous scattering medium as well as the transformations of its time distribution at infinitely growing optical thickness of the medium.

3. Numerical modeling of the signal time structure

It is of primary interest in this study to track the behavior of the ratio between the fraction of radiation scattered at small angles and the diffuse one as a function of the optical thickness of a scattering layer. The time structure of the light field has been calculated using a model of point isotropic source located in a conservative homogeneous scattering medium. Therefore, one can expect that the scattered radiation will become diffuse faster than in the case of a directed beam.

Modeling of the light field was made by means of the Monte Carlo method using the algorithms of the local estimate[51,52] for the time-dependent transfer equation. It is assumed that a point source $P_0(\mathbf{r}, t) = \delta(\mathbf{r})\delta(t)$ with the unity intensity is in a homogeneous medium with the scattering coefficient σ and the scattering phase function $g(\gamma) = \beta(\gamma)/\sigma$ ($\beta(\gamma)$ is the coefficient of directional scattering). At the distance Z from the source (at the point $\mathbf{r} = \mathbf{r}^\circ$), there is placed a point receiver with the cosine directional pattern. The first photons reach the receiver at $T_0 = Z/c$.

The Monte Carlo method is based on RTE solution in the integral form by its expansion into the iterative series. For the flux vector, $\mathbf{F}(\mathbf{r}) = \int\limits_{4\pi} I(\mathbf{r},\mathbf{s})\,\mathbf{s}\,d\omega$, this equation has the form[1]

$$\mathbf{F}(\mathbf{r}) = \mathbf{F}_{ri}(\mathbf{r}) + \int\limits_{V}\left[\int\limits_{4\pi}\sigma g(\mathbf{s},\mathbf{s}')I(\mathbf{r}',\mathbf{s}')d\omega'\right]\frac{e^{-\tau}}{|\mathbf{r}-\mathbf{r}'|^2}\mathbf{s}\,dV'. \quad (5)$$

Here $\mathbf{F}_{ri}(\mathbf{r})$ is the vector of attenuated incident radiation flux, $\tau = \varepsilon|\mathbf{r} - \mathbf{r}'|$ is the optical length of the path between the points of scattering and observation. Illumination at the point $\mathbf{r}^\circ$ determined by scattered radiation is calculated as an estimate of a random variable being the sum of the series over collisions:

$$E(\mathbf{r}^\circ) = \int\limits_{2\pi} I(\mathbf{r}^\circ,\mathbf{s}^\circ)\cos\varphi\,d\omega^\circ = M\sum_n l_i(\mathbf{x}_n,\mathbf{x}^\circ),$$

$$l_i(\mathbf{x},\mathbf{x}^\circ) = \frac{e^{-\tau(\mathbf{r},\mathbf{r}^\circ)}g(\gamma^\circ)}{2\pi|\mathbf{r}-\mathbf{r}^\circ|^2}\left|(\mathbf{n}^\circ,\mathbf{s}^\circ)\right|, \quad (6)$$

where $\mathbf{x}_n = (\mathbf{r}_n, \mathbf{s}_n)$ is the point of n-order scattering, $\mathbf{s}^\circ$ is the scattering direction leading the photon to the point of the receiver, $\mathbf{n}^\circ$ is the normal to the receiver's plane. In calculating the photon arrival time to the receiver for each term of the series (6), one can obtain the signal power $P(t)$ (or, in other terminology, the photon distribution over free paths $l = ct$), having in mind that, $E = \int\limits_{T_0}^{\infty} P(t)\,dt$. In our calculations, time axis was uniformly divided, on the logarithmic scale, into the intervals with 5 points per

decade that allowed the fine time structure to of radiation be revealed both at short and long times.

It is worth considering the details of modeling radiation from an isotropic source in media with strongly anisotropic scattering. As follows from physics of the problem, at not so large optical depth, delay time is insignificant and the main contribution to illumination comes from the photons, originally escaped from the source along the directions close to that toward the receiver.

Under these conditions, taking the emission angles equiprobable over the entire sphere, leads to underestimate of the signal and increase in its variance at the initial moments in time. Therefore, this makes it necessary in modeling the initial escape directions, to provide preference to photons escaping from source at small-angles, by introducing the corresponding initial weight of the photon (see, for example, Ref. 53). As shown in Ref. 54, reduction of the calculated intensity variance in this case is connected with the increase in the number of trajectories contributing to the intensity at the initial moments in time.

Besides, under conditions of large optical depth ($\tau > 10$) one has to avoid calculating the low-order scattering of the photons escaped (or scattered) toward the receiver by use of a standard "physical" modeling of the free path l with the distribution density $p_l(x) = \varepsilon\exp(-\varepsilon x)$.[51] In this case the main contribution to the signal intensity comes from photons that undergo collisions in the near vicinity of the receiver. Thus modeling of scattering in this region should have enough statistics. Usually, the optical thickness is set by the formula $\tau = -\ln\alpha$, where α is the random variable, that at a reasonable number of trajectories ($N < 10^9$) does not allow obtaining an adequate statistics at optical thickness more than 10. In using the generators of random numbers in the computer codes like INTEGER*4 based on integer operations does not allow obtaining the optical thickness $\tau > 21$, in principle. Therefore, in modeling low-order collisions (from the first to the fourth), uniform modeling is used for the photon travel path from the point of previous collision to the receiver while introducing the corresponding weight. Otherwise, a considerable underestimate of radiation intensity (by about three orders of magnitude) occurs for the initial moments in time.

The algorithms proposed have already been approbated[54,56] for the control of optical monitoring equipment working in the water medium with essential absorption. In this study, the calculations were made for the conservative medium ($\kappa = 0$), since in this case, the diffusion fraction of radiation manifests itself much stronger. For comparability with data from previous studies four types of seawater scattering phase function are used as earlier, in modeling the scattering medium, which are characterized by a rather high variability of the asymmetry parameter.

The scattering phase functions used were measured by experiment in different time by

O.V. Kopelevich and V.M. Pavlov.[32] Two scattering phase functions have an extreme asymmetry. The least forward peaked scattering phase function g_1 ($<\cos\gamma> = 0.788$) was observed in clear waters of the Sargasso Sea, the most forward peaked one g_4 ($<\cos\gamma> = 0.987$) in waters of the Black Sea. Scattering phase functions g_2 ($<\cos\gamma> = 0.924$) and g_3 ($<\cos\gamma> = 0.97$) are typical for waters in the open ocean. Besides, the molecular scattering phase function g_m was used, as well. The majority of natural water media have significant absorption, and the number of photons with large free paths will be strongly attenuated according to the well-known relation[4]:

$$P(t, \sigma, \kappa \neq 0) = P(t, \sigma, \kappa = 0)\exp(-\kappa ct).$$

It should be noted that results presented in this paper have been obtained in setting the stationary value of $\sigma = 0.15$ m^{-1} and variable distance Z between the source and the receiver. In calculations, I took from 10 up to 200 millions of trajectories depending on the type of the scattering phase function and position of the time interval on the time axis.

4. Calculated results

Let us consider the region of small optical thickness (about unity), at which low-order scattering and small level of diffuse background are assumed. Figures 2 and 3 present the distribution over free paths of the photons emitted from the point isotropic source in the infinite, homogeneous, and conservative scattering medium. Abscissa shows the photon time delay Δt relative to the arrival time of the first photon (total $t = T_0 + \Delta t$). Figure 2 shows pulse deformation at an increase of the distance from the source to the receiver from $Z = 0.2$ m ($\tau = 0.03$) up to $Z = 30$ m ($\tau = 4.5$) for the medium with g_2. Figure 3 presents the dependences for different scattering phase functions and the distance $Z = 5$ m ($\tau = 0.75$).
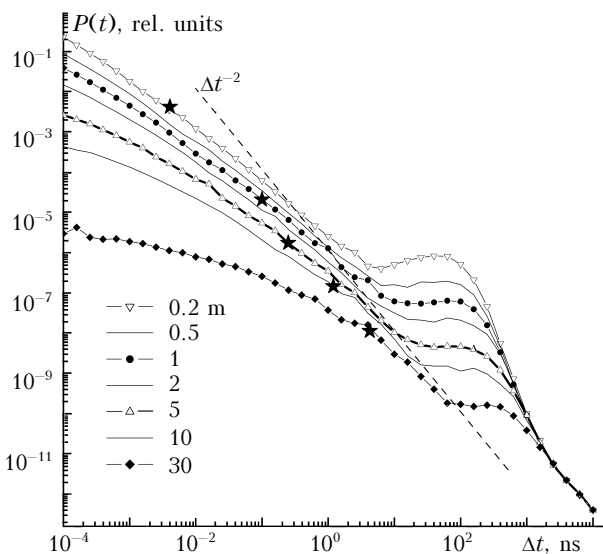

Fig. 2. Pulse shape for the medium with g_2 and different distances Z.

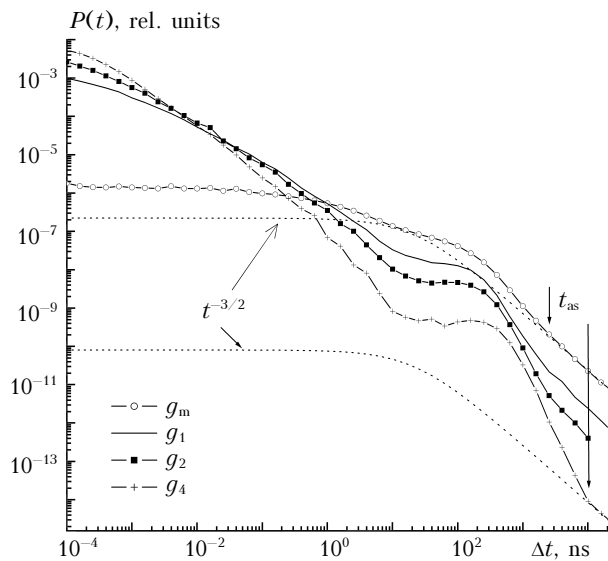**Fig. 3.** Pulse shape for different scattering phase functions and $Z = 5$ m.

It is clear that the distribution is a curve with two maxima. The first delta-shaped peak is caused by the small-angle scattering at the initial moments in time that does not lead to any considerable increase of the photon free path. Increasing delay time causes an increase in the curve slope, approaching the "pseudoasymptotic" with the slope obeying Δt^{-2} law. Then, the second maximum formed by photons appears. Delay time of these photons much exceeds the travel time T_0. It is for sure that here dominate the photons scattered at large angles. Stars on the curves (see Fig. 2) show the moments at which a half of the scattered radiation energy comes. At the moment the second maximum occurs, for all distances and g_2 scattering phase function, about 85–90% of scattering energy comes.

At a large time, distribution takes the asymptotic dependence typical for the isotropic source in the infinite medium[6] $P(t) \sim t^{-3/2}$ (dotted line in Fig. 3) and statistical modeling for the later moments makes no sense since the pulse shape can be calculated analytically. The moments t_{as} of approaching the asymptotic are shown by the arrows in the right-hand part of the curves. In the case of strongly forward peaked scattering phase functions approaching the asymptotic occurs later compared to that in the case of less asymmetric ones. The values of the dimensionless time $u = \sigma ct$ at t_{as} are 80 for g_m and 340 for g_4. A fraction of energy coming after t_{as}, is higher for slightly asymmetric scattering phase functions (both absolutely and relatively): it is 3.7% for molecular, 0.5% for g_1 and only 0.002% for g_4 scattering phase functions. For media with nonzero absorption, this residual energy is negligible.

Figure 4 for $Z = 5$ m shows energy $E^t =$

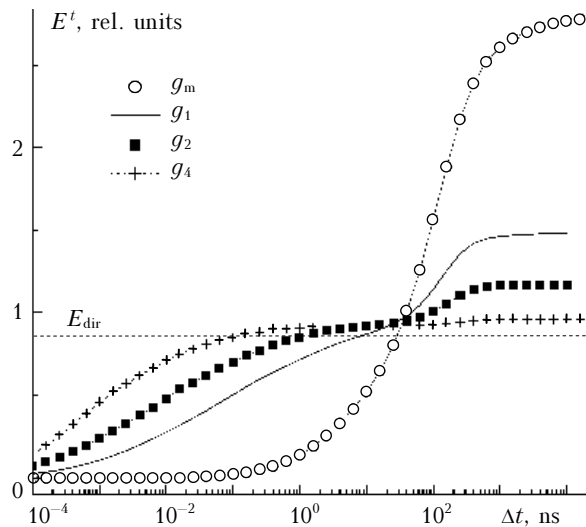$$= \int_{T_0}^{t} P(t)\,dt$$ accumulated by the time t.

Fig. 4. Energy of the scattered radiation ($Z = 5$ m) accumulated by the moment $T_0 + \Delta t$ in media with different scattering phase functions.

Horizontal dot line denotes energy of attenuated direct beam. The growth of piled up energy occurs in two steps. The first rapid energy increase occurs in the initial moments in time due to then dominating scattering at small angles. The second one, "diffuse" maximum in $P(t)$ distribution leads to the new considerable energy increase, moreover, this addition of scattered radiation is comparable with the direct beam energy E_{dir}. The two-scale time structure in pulse energy is especially evident in media with the medium asymmetric scattering phase functions ($g_1 - g_3$). There is a time interval between the maxima for such scattering phase functions (here $\Delta t \approx 10$ ns is the delay comparable with the time of photon travel along the path), when no energy pile up occurs. Thus by this moment in the medium with g_4, already 96% of energy passes whereas for g_m — only 25%.

Now let us consider the transformation of pulse time structure at further increase in optical thickness. Figure 5 shows the pulse form transformation for the medium with g_3 for the optical thickness range from $\tau = 1.5$ ($Z = 10$ m, curve 1) up to $\tau = 150$ (1000 m, curve 6). The dotted curves $4'-6'$ for the corresponding optical thickness show the pulse form in DA (3).

First of all, one should notice the gradual smoothing and disappearance of the delta-shaped peak (it characterizes the range of transient optical thickness values) at the optical thickness increasing up to the values of 10–15 (curves 2, 3). Hence, a new maximum with a finite value of $t_{max} \neq 0$ is formed. The small-angle scattering still may play the main role in this value but its duration is already determined and can be measured in the experiment. We shall point out once more that the delta-shaped peak observed in the initial moments in time at small distances, has no duration in terms of the pulse width at half-maximum. The ratio between amplitudes and

duration of maxima due to small-angle and diffuse scattering at $\tau = 15$ makes some orders of magnitude and they cannot be measured in the experiment simultaneously. It is just this circumstance that introduces ambiguity to the measurements in the region of transient optical thickness. At $\tau = 30$ (curve 4), the delta-shaped peak completely disappears. However, DA (dot line $4'$) even at this optical thickness describes the height and shape of the distribution quite wrongly.
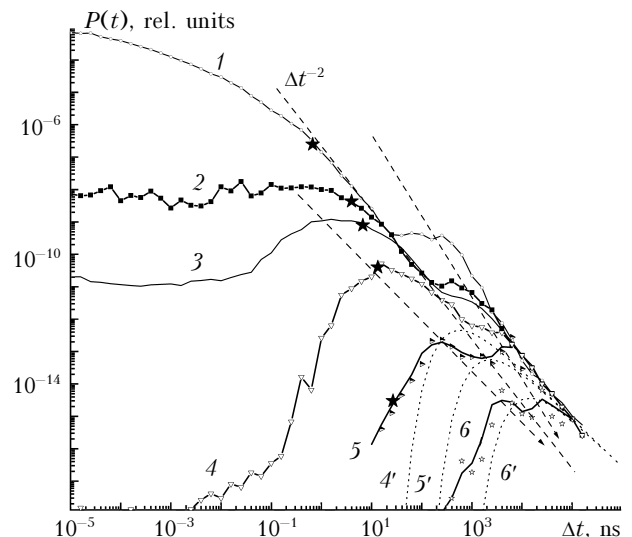

Fig. 5. Pulse shape for the entire range of optical thickness values and g_3. Curve 1 is $Z = 10$ m ($\tau = 1.5$); 2 is 60 ($\tau = 9$); 3 is 100 ($\tau = 15$); 4 is 200 ($\tau = 30$); 5 is 400 ($\tau = 60$); 6 is 1000 ($\tau = 150$).

Thus, there are two maxima in photon distribution over free paths for the point radiation source starting with the region of transient optical thickness ($\tau = 10$–15). Each of these maxima moves, at increasing optical thickness to the region of longer times and its amplitude decreases. The maximum shift for the first peak is faster than that determined by the quadratic dependence for DA (4), whereas diffuse maximum, on the contrary, sifts slower. The position of the inflection point between the peaks (see the dashed line Δt^{-2} in Fig. 5) best corresponds to the dependence according to formula (4). As a result, the two peaks gradually become closer as τ increases and for $\tau = 150$ (curve 6), the peaks almost merge. From this very optical thickness DA (curve $6'$) describes the photon distribution over free paths satisfactorily, although, the distribution excess over the diffusion one is still noticeable on its short-time side. We shall remind that DA applicability is determined by large value of transport optical thickness $\tau_D = \tau(1 - \langle\cos\gamma\rangle)$, which for $Z = 1000$ m and g_3 (($1 - \langle\cos\gamma\rangle) = 0.03$) makes 4.5. One can count that it considerably exceeds the unity. Respectively, for the scattering phase functions with lower asymmetry, the peaks merge at smaller optical thickness and DA becomes valid earlier.

Some words are to be said on the validity and conditional character of the interpretation proposed in this paper of the maxima in $P(t)$ distribution as being formed by radiation scattered at small angles and by the diffuse radiation. Predominance of the small-angle scattering is obvious enough in media with forward peaked scattering phase function at small optical thickness and in the initial moments in time, but at $\tau \approx 10$, it requires refinement. Elongation of the photon free path at $\theta \ll 1$ is less than the entire path length and makes value $\Delta t_s \approx T_0 \theta^2/2$. In Fig. 5, stars mark the Δt_s, corresponding to the scattering angle $10°$ ($\theta^2/2 = 0.015$).

One can consider that up to $\tau = 15$ (curve *3*), the first maximum is completely formed by the radiation scattered at small angles $\theta < 10°$. The large-angle scattering plays the main role in the first maximum at large distances. It leads to gradual wash out of the bimodal structure. At the same time, "diffuse" maximum cannot be uniquely interpreted as a completely formed diffuse background, where the photons forget the initial direction they were emitted along. At small τ,[55] the determining contribution comes, within this time interval, from the low-order scattering from the hemisphere behind the source to the angle close to $180°$. The DA[50] also shows the effect of scattering medium geometry on the pulse broadening.

It is known that for the semi-infinite medium (the radiation source is at the medium boundary, and the receiver is in the medium depth), asymptotic drop is described by the dependence $t^{-5/2}$ (Ref. 6), whereas for the infinite medium — by the $t^{-3/2}$ dependence. At $\tau = 15$, the distribution shape for these two cases is shown in Fig. 6 (scattering phase function g_3).
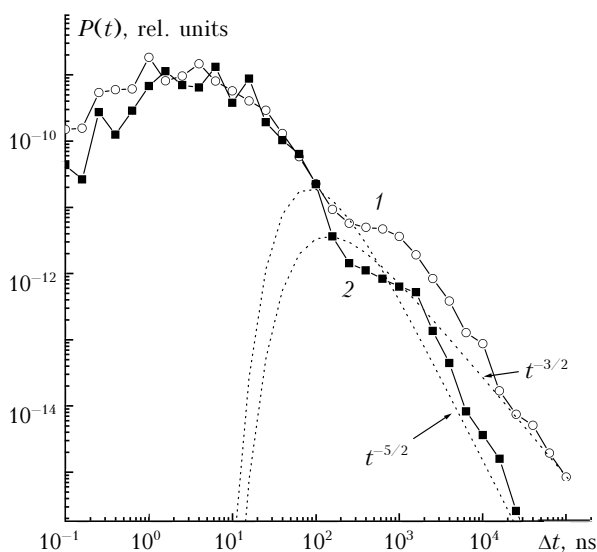

Fig. 6. Distribution over free paths for infinite (*1*) and semi-infinite (*2*) medium. Scattering phase function g_3, $\tau = 15$.

Illumination for the semi-infinite layer (curve *2*) in the whole time interval is expressed through the corresponding signal for the infinite medium as $P(t) = P^\infty(t)T_0/t$, that agrees with results of diffusion theories.[6,16] It is characteristic that diffuse maximum amplitude (at $\Delta t = 600$ ns) falls down for the semi-infinite medium by 5 times, hence, the main contribution comes from the opposite hemisphere (with respect to the receiver) behind the source. Thus real diffuse mode, when the photons forget the place of their origin, has not been formed at $\tau = 15$, and DA (dot line) describes neither small-angle nor diffuse maxima. It also should be noted here that pulse duration depends also on the transverse dimensions of the scattering medium. The calculations by Bucher[30] have shown that at cylindrical cloud geometry (diameter is approximately equal to the distance), pulse duration decreases by 3 to 6 times. Decrease of the duration by 3 times has also been recorded in the experiments by Vergoun[24] in the chamber with the diameter equal to its half-length.

Conclusions

Photon distribution over free paths in the region of small and transient optical thickness ($\tau = \varepsilon Z \gg 1$, but transport optical length $\tau_D = \tau(1 - <\cos\gamma>)$ is not large yet) has the shape of a bimodal curve. At small τ, the first delta-shaped peak is determined by the small-angle scattering, the second one, "diffuse" maximum includes the large-angle scattering. At increase in the optical distance, τ, between the source and the receiver, the position of both maxima and the inflection point between them is moved to the longer times. Consequently, the fraction of energy in the diffuse maximum is determined, first of all, by the scattering phase function asymmetry and weakly depends on τ.

In the region of transient optical thickness, there is an ambiguity in measurements of the pulse duration due to limited dynamic range of photo detectors and different ratios between time resolution of the equipment and the length of the measurement path. At further increase in optical thickness, the ambiguity disappears since the maxima positions become closer, and at $\tau = 150$ ($\tau_D = 4.5$) they are merged into a single maximum. The shape of this maximum is satisfactorily described by DA.

Acknowledgments

References

1. A. Ishimaru, *Wave Propagation and Scattering in Random Media.* Vol. 1. *Single Scattering and Transport Theory* (Academic Press, New York, 1978).

2. E.P. Zege, A.P. Ivanov and I.L. Katsev, *Image Transfer in Scattering Medium* (Nauka i Tekhnika, Minsk, 1985), 327 pp.

3. V.V. Sobolev, *Light Scattering in Planetary Atmospheres* (Nauka, Moscow, 1972), 335 pp.

4. A.P. Ivanov, *Principal Physics of Hydrooptics* (Nauka i Tekhnika, Minsk, 1975), 503 pp.

5. I.N. Minin, Vestn. Len. Univ., No. 3, 131–141 (1959).

6. E.P. Zege and I.L. Katsev Dokl. Belarus. Akad. Nauk **13**, No. 8, 254–260. (1969).

7. L.M. Romanova, Izv. Akad. Nauk SSSR, Fiz. Atmos. Okeana **6**, No. 5, 489–498 (1970).

8. L.S. Dolin, Izv. Akad. Nauk SSSR, Fiz. Atmos. Okeana **16**, No. 1, 55–64 (1980).

9. L.B. Stotts, J. Opt. Soc. Am. **67**, No. 6, 815–819 (1977).

10. S. Chandrasekhar, Rev. Mod. Phys. **15**, No. 1, 1–89 (1943).

11. V.F. Weiskopf, in: *Science and Engineering of Nuclear Power*, C. Goodman, ed. (Cambridge, Addison-Wesley, (1947), pp. 87–97.

12. V.V. Smelov, *Lectures on Neutron Transfer Theory* (Atomizdat, Moscow, 1978), 216 pp.

13. E.P. Zege, I.L. Katsev, and I.D. Sherbaf, Izv. Akad. Nauk SSSR, Fiz. Atmos. Okeana **9**, No. 9, 937–946 (1973).

14. V.V. Ivanov and S.D. Gutshabash, Izv. Akad. Nauk SSSR, Fiz. Atmos. Okeana **10**, No. 8, 851–863 (1974).

15. A. Ishimaru, J. Opt. Soc. Am. **68**, 1045–1050 (1978).

16. S. Ito and K. Furutsu, J. Opt. Soc. Am. **70**, No. 4, 366–374 (1980).

17. K. Furutsu, J. Opt. Soc. Am. **70**, No. 4, 360–366 (1980).

18. S. Ito, J. Opt. Soc. Am. **1**, No. 5, 502–505 (1984).

19. A.P. Chievro, Appl. Opt. **34**, No. 30, 7137–7148 (1995).

20. R.F. Bonner, R. Nossal, S. Havlin, et al., J. Opt. Soc. Am. **4**, No. 3, 423–432 (1987).

21. L.S. Dolin, Izv. Akad. Nauk SSSR, Fiz. Atmos. Okeana **19**, No. 4, 400–404 (1983).

22. V.S. Remizovich, D.B. Rogozkin, M.I. Ryazanov, et al. Izv. Akad. Nauk SSSR, Fiz. Atmos. Okeana **19**, No. 10, 1053–1061 (1983).

23. D.B. Rogozkin, Izv. Akad. Nauk SSSR, Fiz. Atmos. Okeana **23**, No. 4, 366–375 (1987).

24. V.V. Vergun, E.V. Genin, G.P. Kokhanenko, et al., Atm. Opt. **3**, No. 9, 845–851 (1990).

25. V.V. Vergun, M.V. Kabanov, G.P. Kokhanenko, et al., Dep. VINITI, Reg. No. 5645-84, July 20, 1984, Moscow (1984), 20 pp.

26. I.L. Katsev, Dokl. Belarus. Akad. Nauk **13**, No. 2, 118–121 (1969).

27. J.W. McLean, J.D. Freeman, and R.E. Walker, Appl. Opt. **37**, No. 21, 4701–4711 (1998).

28. R.F. Lutomirski, A.P. Chievro, and G.J. Hall, Appl. Opt. **34**, No. 30, 7125–7136 (1995).

29. G.M. Krekov, G.A. Mikhailov, and B.A. Kargin, Izv. Vyssh. Uchebn. Zaved., Fizika, No. 5, 54–59 (1968).

30. E.A. Bucher, Appl. Opt. **12,** No**.** 10, 2391–2400 (1973).

31. R.M. Lerner and J.D. Summers, Appl. Opt. **21**, No. 5, 861–869 (1982).

32. A.M. Gourfink, in: *Oceanic Light Fields* (Optical Institute, Akad. Sciences SSSR, Moscow, 1980), pp. 115–165.

33. A.K. Zakharov and Yu.A. Goldin, Izv. Akad. Nauk SSSR, Fiz. Atmos. Okeana **22**, No. 5, 533–540 (1986).

34. V.V. Korshunov, Atm. Opt. **3**, No. 11, 1047–1051 (1990).

35. G.P. Kokhanenko and V.A. Krutikov, in: *Abstracts of Reports* (Publishing House of the Academy of the ESSR, Tartu, 1988), pp. 98–101.

36. E.A. Bucher and R.M. Lerner, Appl. Opt. **12**, No. 10, 2401–2414 (1973).

37. V.V. Korshunov, L.N. Pavlova, N.P. Romanov, et al., Izv. Ros. Akad. Nauk, Fiz. Atmos. Okeana **30**, No. 1, 39–45 (1994).

38. W.H. Paik, M. Tebyani, D.J. Epstein, et al., Appl. Opt. **17**, No. 6, 899–905 (1978).

39. G.C. Mooradian and M. Geller, Appl. Opt. **21**, No. 9, 1572–1577 (1982).

40. G.C. Mooradian, M. Geller, L.B. Stotts, et al., Appl. Opt. **18**, No. 4, 429–441 (1979).

41. R.A. Elliott, Appl. Opt. **22**, No. 17, 2670–2681 (1983).

42. J.C. Matter and R.G. Bradley, Appl. Opt. **20**, No. 13, 2220–2229 (1981).

43. V.K. Gavrikov and V.G. Korenev, Izv. Akad. Nauk SSSR, Fiz. Atmos. Okeana **17**, No. 7, 763–765 (1981).

44. V.N. Pelevin, A.M. Gourfink, and Yu.A. Goldin, Okeanologiya **19**, No. 2, 228–232 (1979).

45. Yu.A. Goldin, V.A. Gashko, G.G. Karlsen, et al., in: *Hydrophysical and Hydrooptical Studies in Atlantic and Pacific Oceans* (Nauka, Moscow, 1974), pp. 228–241.

46. K. Shimizu and A. Ishimaru, Opt. Lett. **5**, No. 5, 205–207 (1980).

47. V.V. Vergun, M.V. Kabanov, G.P. Kokhanenko, et al., Opt. Atm. **1**, No. 2, 97–99 (1988).

48. H. Leelavathi and J.P. Pichamuthu, Appl. Opt. **27**, No. 12, 2461–2468 (1988).

49. V.C. Hulst, Bull. Astron. Inst. Netherlands **20**, 77–85 (1968).

50. S. Ito, Appl. Opt. **20**, No. 15, 2706–2715 (1981).

51. G.I. Marchuk, G.A. Mikhailov, M.A. Nazaraliev, et al., *Monte-Carlo Method in Atmospheric Optics* (Nauka, Novosibirsk, 1976), 284 pp.

52. G.M. Krekov, G.A. Mikhailov, B.A. Kargin, et al., Izv. Vyssh. Uchebn. Zaved., Fizika, No. 4, 5–9 (1968).

53. M.N. Gorshkov and M.A. Nazaraliev, in: *Monte-Carlo Methods in Computing Mathematics and Mathematical Physics* (Novosibirsk, 1979), pp. 5–14.

54. G.P. Kokhanenko, B.A. Tarashchansky, N.M. Budnev, et al., Proc. SPIE **6160**, 64–76 (2005).

55. N.M. Budnev, G.P. Kokhanenko, M.M. Krekova, et al., Atmos. Oceanic Opt. **18**, Nos. 1–2, 96–104 (2005).

56. N.M. Budnev, G.P. Kokhanenko, R.R. Mirgazov, et al., Atmos. Oceanic Opt. **19**, No. 4, 314–321 (2006).